Acta Oceanol. Sin., 2017, Vol. 36, No. 12, P. 111–118
DOI: 10.1007/s13131-017-1074-3
http://www.hyxb.org.cn
E-mail: hyxbe@263.net

Impact of Phase III Project of Maji Mountain Port on sediment siltation in adjacent sea area

JIN Zuowen[1, 2], ZUO Changsheng[3], WANG Zhizu[4*]

[1] College of Oceanic and Atmospheric Sciences, Ocean University of China, Qingdao 266100, China

[2] East China Sea Branch of State Oceanic Administration, Shanghai 200137, China

[3] National Marine Information Center, Tianjin 300171, China

[4] East China Sea Center of Standard and Metrology, State Oceanic Administration, Shanghai 200137, China

Received 21 February 2017; accepted 10 May 2017

Abstract

Based on a 3-D Finite Volume Coastal Ocean Model (FVCOM), tidal dynamics has been studied in the sea area around the Phase III Project of Maji Mountain Port (MMP). Furthermore, taking typhoon "Canhong" as an example, a storm surge and sediment model has also been established to study the impact of the Phase III Project on current flows and siltation during extreme weather. Tidal currents before and after the project have been compared. Model results show that the changes of tidal current mainly occur in the engineering areas with a magnitude change of 0.3–0.4 m/s during maximum flood and ebb tides. The flow condition for the port has been improved as the flow direction is changed to parallel to the wharf after the completion of the project. There is little siltation in the adjacent area, which will not affect the safety of ship navigation. Besides, the sudden siltation during typhoon period is relatively weak. The back silting in two days is less than 5 cm indicating no sudden siltation occurs.

Key words: Maji Mountain Port, FVCOM, tidal current, siltation, storm

Citation: Jin Zuowen, Zuo Changsheng, Wang Zhizu. 2017. Impact of Phase III Project of Maji Mountain Port on sediment siltation in adjacent sea area. Acta Oceanologica Sinica, 36(12): 111–118, doi: 10.1007/s13131-017-1074-3

1 Introduction

The Maji Mountain Port (MMP) is located in the Maji Mountain Island (MMI), which is about 1 500 m to the southwest of the Sijiao Island, Shengsi County, Zhejiang Province (Fig. 1). Geographically, MMP serves as a sea gate and channel of the Changjiang River (Yangtze River) and the Changjiang River Delta region for the world, with great influence to the other Asia-Pacific ports (Wang et al., 2006). It is dominated by semi-diurnal tide, with longer period of falling tide than that of rising tide. The tidal current is mainly rectilinear, and the residual current is small (Zhang and He, 2013). The suspended sediment is mainly from the Changjiang River, Qiantang River, etc., as well as the local resuspension caused by waves and tides (Ji et al., 2015).

Port construction would take effects to the ambient water and sediment environment (Zhang et al., 2014), which has often been reported in previous studies (Fu et al., 2007; Wen and Liu, 2015; Feng et al., 2008; Feng et al., 2008; Liu et al., 2012). To evaluate the impact of ocean engineering on marine environment has become a hot topic (Liu et al., 2016; Liu, 2012b) in coastal countries and regions. Based on field measurements and numerical modelling, this paper aims to explore the impact of the construction of MMP Phase III Project on tidal and sediment dynamics in the adjacent sea area.

2 Data and model configuration

2.1 *Data source*

The water level was collected in five stations (including a temporary tide-level station near the engineering project) with one–month length and 10-min intervals. The tidal current was measured by ten mooring stations and two buoys for a continuous 17-day. In addition, suspended sediment concentration (SSC) was measured at Sta. V4, which located near the Phase III wharf on the west of MMP. For each station, 28-hour data with 1-hour intervals and 6 layers in depth was obtained for model validation during spring, moderate, and neap tides, respectively. The measurement position and period at each station are shown in Tables 1 and 2.

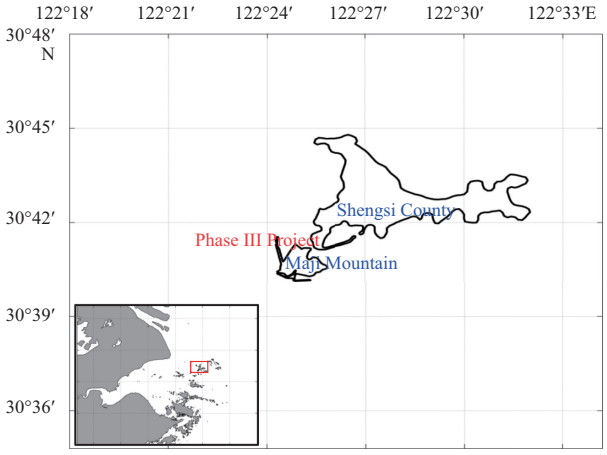

Fig. 1. Location of the MMP and the Phase III Project.

*Corresponding author, E-mail: wzz1104@163.com

Table 1. Information of tidal level stations

Location	North latitude	East longitude	Period
Luchao Port	30°50′24.00″	121°50′42.00″	July 1–31, 2015
Xiaoqu Mountain	30°32′00.00″	122°16′00.00″	
Xiaoyang Mountain	30°38′22.14″	122°02′24.25″	
Maji Mountain	30°41′14.27″	121°25′17.13″	
Temporary Tidal Gauge	30°41′26.59″	122°25′16.55″	

Table 2. Information of tidal current stations

Station	North latitude	East longitude	Period
V1	30°41′17.31″	122°23′34.97″	spring tide: July 1, 2015; July 17–18, 2015 moderate tide: July 5–6, 2015 neap tide: July 8–9, 2015
V2	30°41′04.49″	122°23′37.85″	
V3	30°40′45.46″	122°23′44.41″	
V4	30°40′55.07″	122°23′52.67″	
V5	30°40′32.08″	122°24′00.82″	
V6	30°41′14.27″	122°25′17.13″	
V7	30°43′09.38″	122°24′06.68″	
V8	30°41′01.49″	122°21′56.15″	
V9	30°39′13.67″	122°23′38.93″	
V10	30°37′47.75″	122°26′22.21″	
V11	30°38′55.51″	122°27′49.25″	
V12	30°40′16.24″	122°27′14.97″	

2.2 *Hydrodynamic model*

Based on the unstructured grid, Finite-Volume, primitive equation Community Ocean Model (FVCOM) (Chen et al., 2006), a high-resolution three-dimensional tidal current numerical model for MMP is established. The unstructured triangular mesh can better fit the complicated shoreline of MMP and Zhoushan archipelago. In vertical, the σ-coordinate is used and the coordinate transformation is represented as follows:

$$\sigma=\frac{z-\zeta}{H+\zeta}=\frac{z-\zeta}{D}. \tag{1}$$

The momentum equation, the continuity equation, and the state equation for the model are also given below:

$$\frac{\partial\zeta}{\partial t}+\frac{\partial Du}{\partial x}+\frac{\partial Dv}{\partial y}+\frac{\partial w}{\partial\sigma}=0, \tag{2}$$

$$\frac{\partial uD}{\partial t}+\frac{\partial u^2D}{\partial x}+\frac{\partial uvD}{\partial y}+\frac{\partial uw}{\partial\sigma}-fvD=-gD\frac{\partial\zeta}{\partial x}-\frac{gD}{\rho_0}\left[\frac{\partial}{\partial x}\left(D\int_\sigma^0\rho\mathrm{d}\sigma'\right)+\sigma\rho\frac{\partial D}{\partial x}\right]+\frac{1}{D}\frac{\partial}{\partial\sigma}\left(K_m\frac{\partial u}{\partial\sigma}\right)+DF_x, \tag{3}$$

$$\frac{\partial vD}{\partial t}+\frac{\partial uvD}{\partial x}+\frac{\partial v^2D}{\partial y}+\frac{\partial vw}{\partial\sigma}+fuD=-gD\frac{\partial\zeta}{\partial y}-\frac{gD}{\rho_0}\left[\frac{\partial}{\partial y}\left(D\int_\sigma^0\rho\mathrm{d}\sigma'\right)+\sigma\rho\frac{\partial D}{\partial y}\right]+\frac{1}{D}\frac{\partial}{\partial\sigma}\left(K_m\frac{\partial v}{\partial\sigma}\right)+DF_y, \tag{4}$$

$$\frac{\partial TD}{\partial t}+\frac{\partial TuD}{\partial x}+\frac{\partial TvD}{\partial y}+\frac{\partial Tw}{\partial\sigma}=\frac{1}{D}\frac{\partial}{\partial\sigma}\left(K_h\frac{\partial T}{\partial\sigma}\right)+D\hat{H}+DF_T, \tag{5}$$

$$\frac{\partial SD}{\partial t}+\frac{\partial SuD}{\partial x}+\frac{\partial SvD}{\partial y}+\frac{\partial Sw}{\partial\sigma}=\frac{1}{D}\frac{\partial}{\partial\sigma}\left(K_h\frac{\partial S}{\partial\sigma}\right)+DF_S, \tag{6}$$

$$\rho=\rho(T,\ S), \tag{7}$$

where u and v are horizontal velocity component, w is vertical velocity, T is temperature, S is salinity, ρ is density, f is Coriolisparameter, and ζ is waterlevel.

2.3 *Typhoon model*

In this study, a typhoon model is established through the parameterization equation, in which the wind and pressure field are obtained based on the typhoon center position, the air pressure and the maximum wind speed radius. The pressure is calculated as follows:

$$P=(P_\infty-P_0)\left(1-\frac{1}{\sqrt{1+2\left(r^2/R^2\right)}}\right)+P_0, \tag{8}$$

$$P=(P_\infty-P_0)\left(1-\frac{1}{1+r/R}\right)+P_0, \tag{9}$$

where P_0 is the pressure of the typhoon center, P_∞ is the external pressure, r is the distance between the calculation point and the typhoon center, and R is the maximum wind speed radius.

The typhoon field is composed of gradient wind and basic wind field:

$$\begin{pmatrix}W_x\\W_y\end{pmatrix}=C_1W_1/r\begin{pmatrix}-(x-x_c)\sin\beta-(y-y_c)\cos\beta\\-(x-x_c)\cos\beta-(y-y_c)\sin\beta\end{pmatrix}+C_2\overrightarrow{W}_2, \tag{10}$$

where $W_1=\frac{fr}{2}\left[\left(1+\frac{4(P_\infty-P_0)s^3}{P_0R_0f^2}\right)^{\frac{1}{2}}-1\right]$,

$s=\left[1+(r/R_0)^2\right]^{\frac{1}{2}}$,

$f=2\omega\sin\varphi$,

$\overrightarrow{W_2}=\mathrm{e}^{-2\pi r\times10^{-6}}\begin{pmatrix}V_x\\V_y\end{pmatrix}$.

where V_x and V_y are typhoon center moving component, r refers to the distance between the calculation point and the typhoon center, x_c and y_c are the typhoon center position, x and y are the calculation point position, β is the angle difference between gradient wind and sea surface wind, and C_1 and C_2 are the correction factor.

2.4 *Sedimentation model*

For the silt coast with sediment median diameter less than 0.05 mm, the equation of Liu Jiaju (2012a) is used in this study to calculate the sediment deposition (Xie, 2011):

$$p=\frac{wS_1t}{\gamma_0}\left\{K_1\left[1-\left(\frac{d_1}{d_2}\right)^3\right]\sin\theta+K_2\left[1-\frac{1}{2}\frac{v_1}{v_2}\left(1+\frac{d_1}{d_2}\right)\right]\cos\theta\right\}, \tag{11}$$

where v_1 and v_2 refer to the averaged current velocity before and after the project, respectively.

2.5 *Model settings*

To obtain a more accurate result, the triangle mesh around

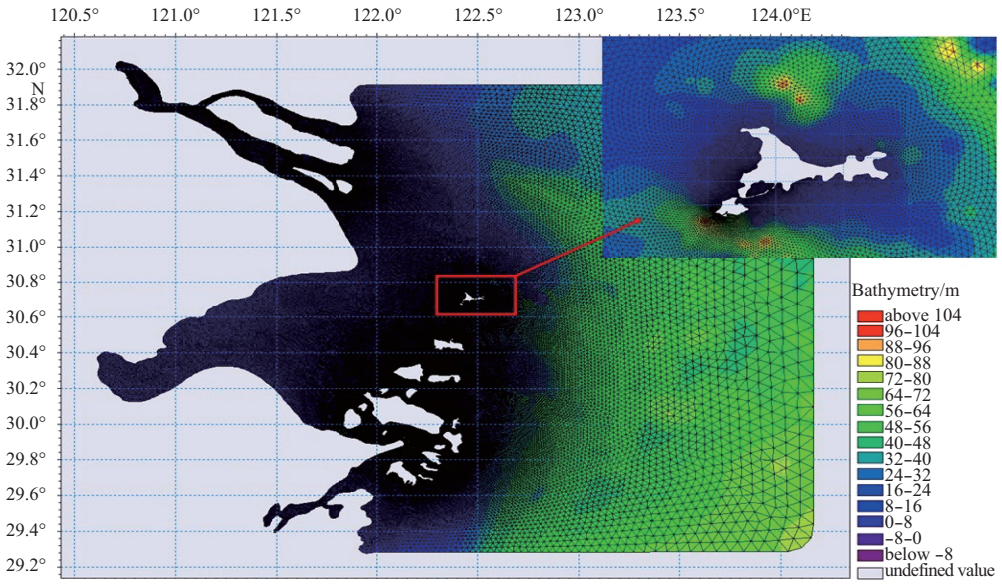

Fig. 2. The computation domain and the mesh grids.

the project should be intensified (Song et al., 2009). Thus, in this study the mesh grid is between 100 m and 200 m around MMI and about 50 m near the Phase III Project. There are in total 84 406 grid nodes and 164 293 mesh cells (Fig. 2) in the computation domain. Six σ-layers are given in vertical. The external time step is set to 0.3 s and the internal mode is 3 s. The bottom drag coefficient is set to be 0.001 m and the water temperature and salinity are given as constant. Zero initial filed for tidal level and tidal flow is used here (Zhu and Cao, 2010). The tidal level at the open boundary is predicted by Tide Model Driver using eight primary constituents (M_2, S_2, K_2, N_2, O_1, K_1, P_1, and Q_1).

2.6 *Model validation*

Two tidal level stations (Xiaoqu Mountain and the temporary tidal gauge) and three tidal current stations (V1, V2, and V3) are chosen to validate the hydrodynamic model. As shown in Fig. 3, the model results capture the observed tidal characteristics and well reproduce the tidal current speed and direction at each station (Fig. 4). The absolute error of the tide current speed and direction is 0.22 m/s and 14°, respectively (Table 3). It indicates the model can be used to study the tidal dynamic in the MMP region, which meets the requirements of the specification (Zhu and Cao, 2010).

3 Impact of Phase III Project on tidal current

3.1 *Changes of tidal current under normal weather*

Figures 5a and b demonstrate the maximum flood and ebb tidal flows in the MMP region before the construction of the project. It indicates that the flood current is larger in front of MMP (south of the MMI) than the other regions, where the current is smaller in the west and north of the island due to the wa-

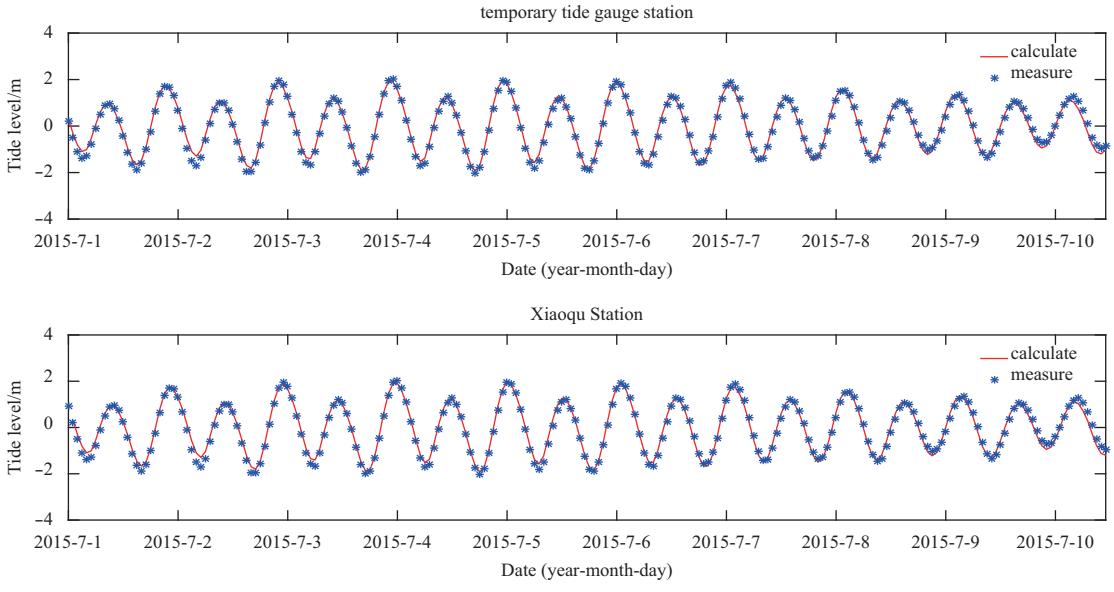

Fig. 3. Comparison between calculated and observed tide levels.

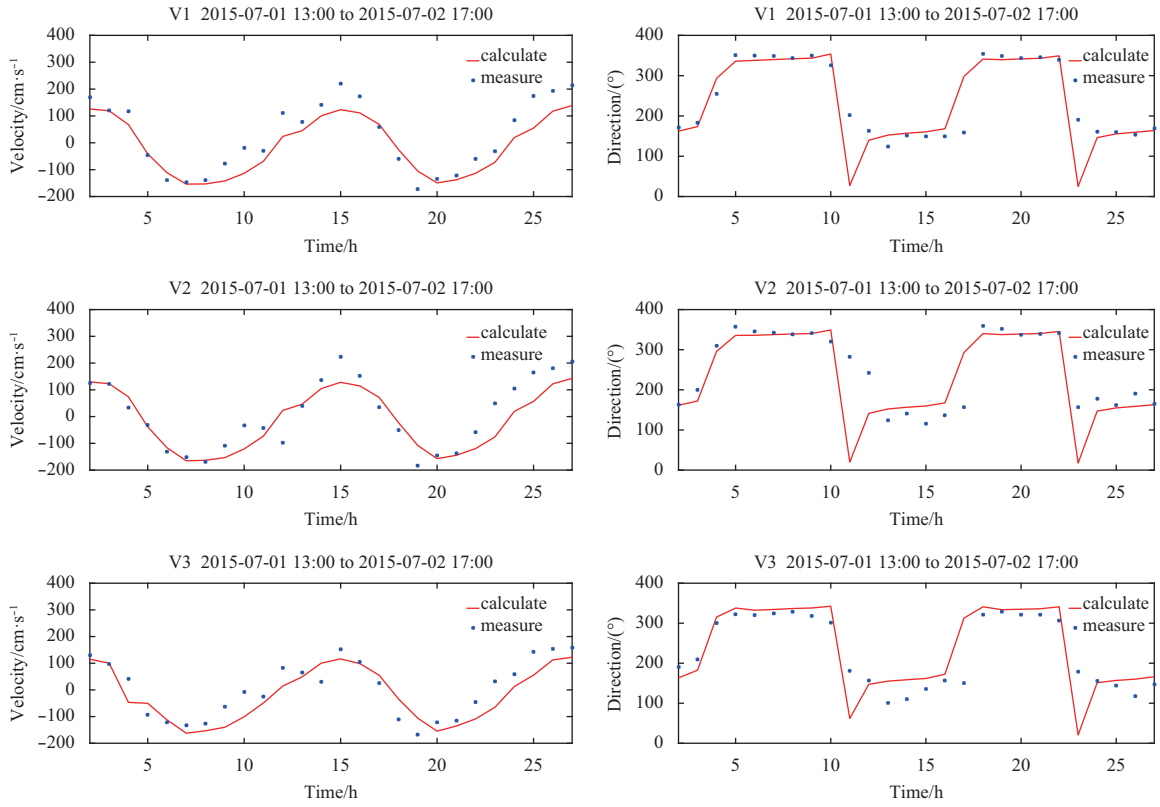

Fig. 4. Comparison between calculated and observed tide current during spring tides.

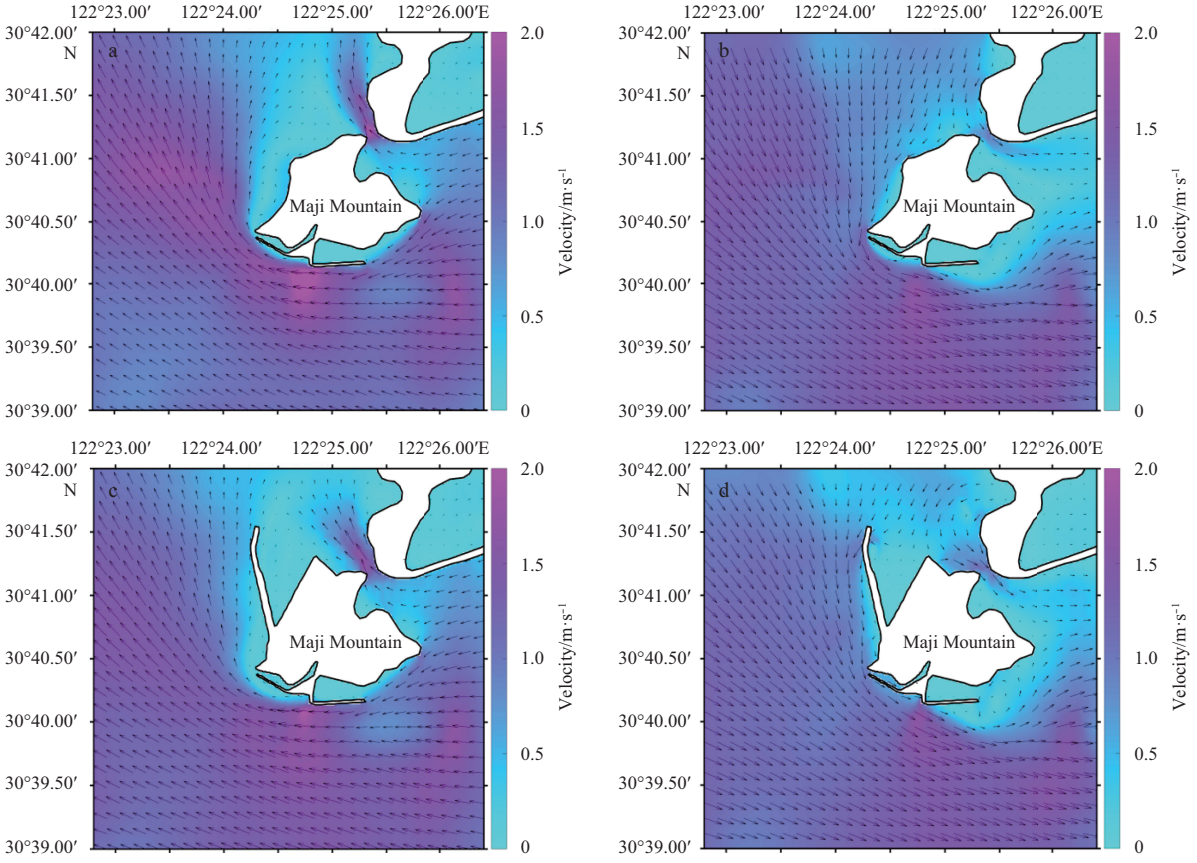

Fig. 5. The tidal current during maximum flood (a) and maximum ebb (b) before the project construction; and that during maximum flood (c) and maximum ebb (d) after the project construction.

Table 3. Errors of tidal current speed and direction

Site	V1		V2		V3	
	Speed/m·s^{-1}	Direction/(°)	Speed/m·s^{-1}	Direction/(°)	Speed/m·s^{-1}	Direction/(°)
Absolute error	0.24	11	0.19	13	0.23	18
Root mean square error	0.20	14	0.17	16	0.18	19

ter depth. It also shows the same distribution for the ebb current. Before the project construction, there is a large angle between the current flow and the coastline in the project area, which was unsafe for the ship berthing (Cui et al., 2008).

In order to study the impact of the Phase III project on the tidal current field in the surrounding sea area, the flow field before and after the project construction is compared. After the project, the maximum flood current increases at the north of wharf due to the project. During ebb tides, the current velocity is reduced due to the wharf blocking. Particularly, the velocity near the wharf is greatly reduced and the flow direction is also changed. After the project, the flow is basically parallel to the wharf.

During spring tides, the averaged velocity on maximum flood is 0.82 m/s before the project; while after the project the average velocity can reach 1.14 m/s with an increase of 0.32 m/s. Before the project, the average velocity on maximum ebb was 0.85 m/s; however, after the project it is only 0.40 m/s, decreased by more than 50%. The changes of tidal current during the moderate and neap tides are consistent with that during the spring tides, but have a smaller magnitude. In general, the tidal current has only significant changes near the wharf, but little in other region around the MMI.

3.2 *Changes of current during the typhoon "Canhong"*

In this section, numerical simulations are carried out to study the change of the current field in the surrounding waters of MMI during a storm, and to provide a dynamic background for the siltation problem.

To examine the impact of typhoon on tidal levels and currents in MMP ambient water, the situation during typhoon "Canhong" is simulated. The typhoon data is obtained online, and interpolated to hourly typhoon center position. Thus, the wind and pressure field can be obtained via Eqs (8)–(10).

Figures 6a and b show the temporal and spatial changes of current during the typhoon before the Phase III Project. It illustrates that when the typhoon is centered on the south of Zhoushan Islands, the easterly wind prevails in the Shengsi area. Under this circumstance, when the astronomic tidal current is large, the current speed close to the Phase III Project can reach up to 2 m/s, which is doubled compared to that under the normal weather conditions.

Figures 6c and d display the spatial and temporal changes of current during the typhoon after the project. It shows that the flow velocity in the inner bay formed by the wharf and the island is rather small during the entire storm, which is decreased by

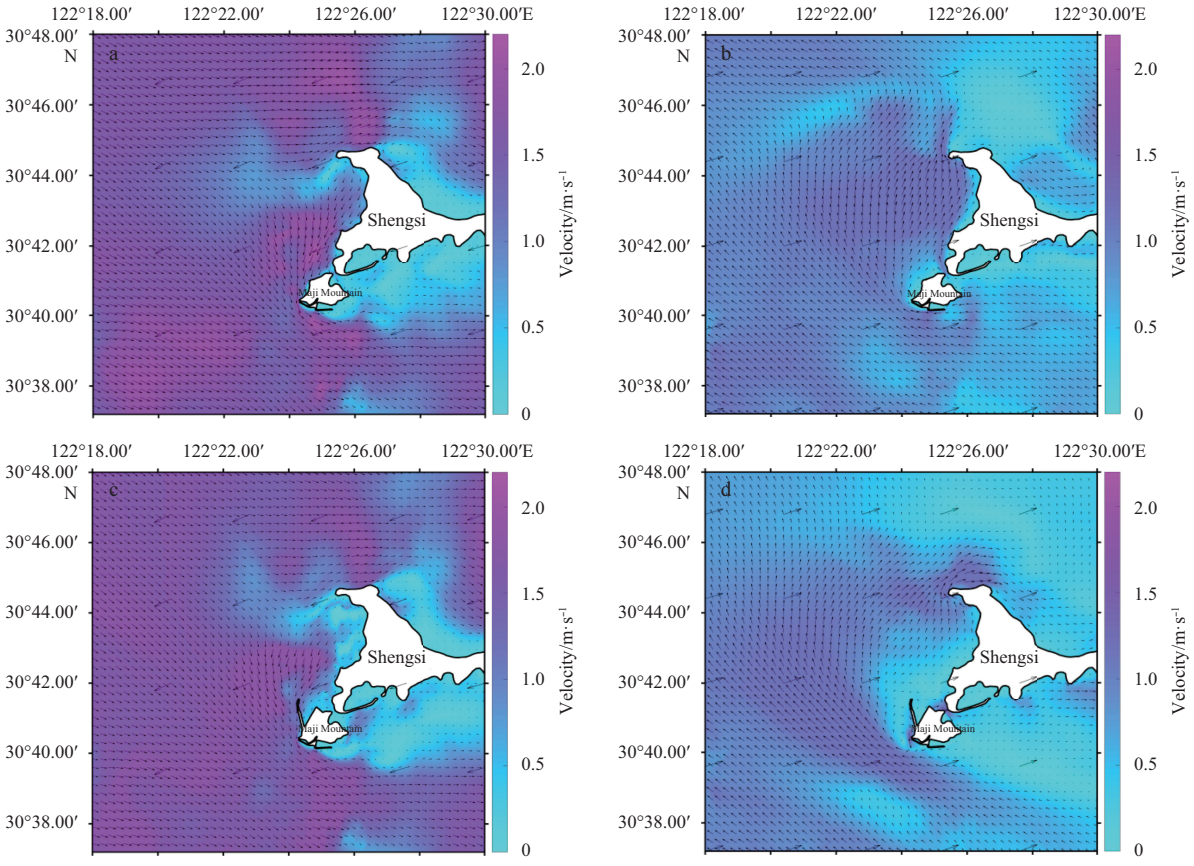

Fig. 6. The wind and current during storm at 06:00 on 11 July 2015 before the construction (a); at 00:00 on 12 July 2015 before the project (b). Figures 6c and d are the same time as Figs 6a and b, respectively, but after the project.

about 1–2 m/s compared to that before the project. While outside the wharf, the current speed is also reduced by about 0.5 m/s. In general, the impact of typhoon on the current in Shengsi sea area is significant, but the impact of MMP Phase III Project is limited only in the port region.

4 Impact of Phase III Project on sedimentation

4.1 *Parameters for sedimentation model*

(1) Settling velocity

The median particle size of suspended sediment collected in the MMP water is 0.005–0.007 mm, categorized as mud. Previous studies indicate that, in this case, flocculation happens in the deposition process, with an equivalent diameter of the flocculation group be 0.015–0.030 mm. Thus, the corresponding settling velocity is 0.01–0.06 cm/s and the value of 0.04 cm/s is used in this study.

(2) SSC

According to the observation, the vertical distribution of SSC is low at surface layer and high at bottom layer. During flood tides, the averaged SSC is 0.054–0.069 kg/m^3 in the surface, 0.148–0.230 kg/m^3 at the 0.6H, and 0.311–0.380 kg/m^3 on the bottom. During ebb tides, the averaged SSC is 0.052–0.065 kg/m^3 in the surface, 0.146–0.183 kg/m^3 at the 0.6H, and 0.286–0.335 kg/m^3 on the bottom. Thus, the averaged vertical SSC is given 0.173 kg/m^3 in this study.

(3) Dry weight of sediment

To calculate the dry weight of sediment, the following method is used:

$$\gamma_0 = 1\,750 D_{50}^{0.183}, \tag{12}$$

where D_{50} is the suspended particle median diameter (mm). According to the suspended sediment sampling in MMP, the average median diameter in spring, moderate, and neap tides are 0.005 1 mm, 0.006 5 mm and 0.005 9 mm, respectively. The D_{50} is thus taken as 0.0058 5 mm in this study and γ_0 is 683 kg/m^3 based on above equation.

(4) The other parameters

The deposition coefficient k is set to 0.13 and the model is run for one-year to calculate the sedimentation rate.

4.2 *Calculation of sedimentation rate*

Figure 7 shows the annual sedimentation intensity after the project construction. As mentioned above, the current on the north of wharf and the west of MMI has been largely reduced. Therefore, siltation mainly occurs in the area.

In the inner bay, located on the west of MMI and north of the wharf, k1–k6 are the main siltation areas with a sedimentation intensity of about 0.2–0.4 m/a. From the wharf to the south, the sedimentation intensity is gradually decreased from 0.1–0.2 m/a to none. And in the region of k13–k20 south of the wharf, the local erosion occurs with an intensity of about 0.05 m/a. In general, the siltation intensity in the MMP region is relatively small, and some areas even have slightly scouring.

It can be seen that the Phase III Project has a certain influence on the marine environment. The current velocity in front of the wharf is higher than that before the project. However, the scouring rate is relatively small and will be balanced by the gradual adjustment of the water flow (Wang, 2014). Siltation mainly occurs on the north of the project. Considering that this region is not a channel, siltation will not affect the navigation safety. But it is still recommended to track and monitor the siltation in this area and further adjustment might be done in future schemes.

4.3 *Sudden siltation in MMP during storm*

In the case of storms, the SSC in muddy coast can be obtained from the following equations (Liu, 2012a):

$$S_2 = 0.027\,3\gamma_s \frac{(|V_m|+|V_n|)^2}{g d_b}, \tag{13}$$

$$V_n = \frac{1}{2}\left(\frac{gH_b^2}{d_b}\right)^{1/2}, \tag{14}$$

where V_m is the averaged current speed during storm, V_n is the average speed of breaking waves, H_b is the breaking wave height, d_b is the depth of breaking wave, γ_s is the sediment particle density which normally is 2 500–2 800 kg/m^3 and is taken as 2 650 kg/m^3 in this study.

During the typhoon "Canhong", H_b and d_b is given 3 m and 10 m, respectively. The other parameters are the same as normal weather conditions. The model is run for 2 d under the extreme weather. The averaged SSC during the storm can reach 8.5 kg/m^3, i.e., the S_2 in Eq. (13), which will be taken into Eq. (11) to calculate the siltation intensity caused by storm.

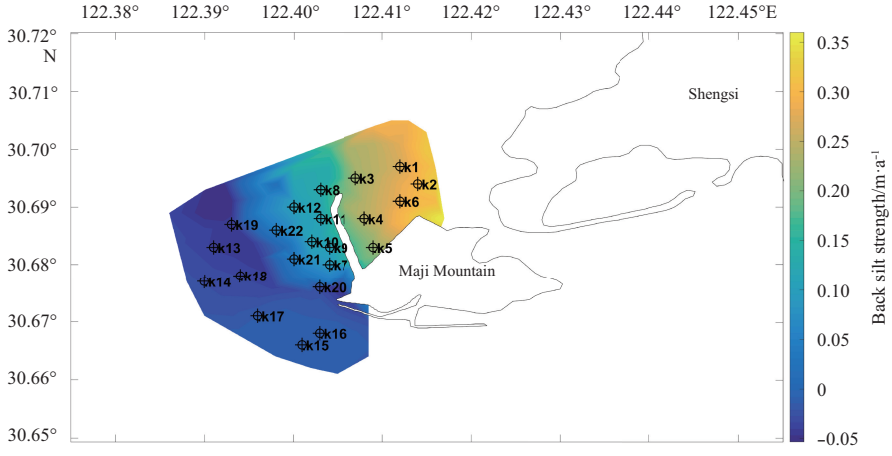

Fig. 7. Distribution of annual back silt strength in Phase III Project of MMP.

As shown in Fig. 8, it indicates that the overall siltation is relatively small during the typhoon, with the siltation decreasing gradually from northeast to southwest. The relatively server siltation problem happens northeast of the wharf.

Figure 8 also shows that the sedimentation rate at k1–k6 northeast of the wharf is relatively large, and the deposited sediment in 2 d can reach about 3–4 cm. While the sedimentation rate at k7–k22 southwest of the wharf is very small, with a thickness of 0–2 cm in 2 d.

The model results indicate that during the typhoon, the key factors of siltation in MMP waters are the increase of storm generated SSC and the change of water flows. The maximum siltation rate in MMP waters is only 4–5 cm in 2 d during the typhoon, and this will not cause sudden siltation.

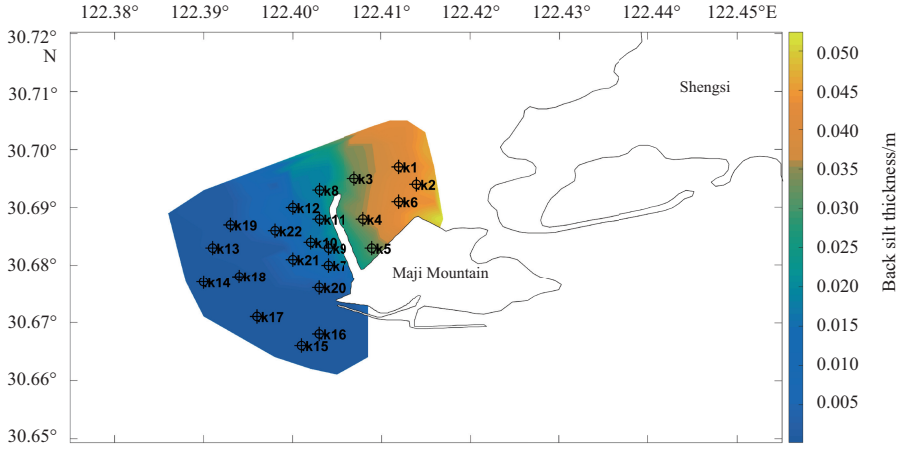

Fig. 8. Distribution of siltation intensity caused by a 2-day storm in MMP waters.

5 Conclusions

For the Zhoushan MMP Phase III Project, a 3-D tidal flow model was established based on FVCOM to study the change of tidal current and sediment siltation before and after the port construction. The results are concluded as follows:

The MMP Phase III Project has little impact on Phase I and Phase II parts. Significant changes on tidal current only occur in the project region. The flood current in the southwest of the wharf has been increased by 0.3 m/s, but the ebb current has been decreases by 0.4 m/s in average. The angle between the current direction and the wharf is basically within 10°. The port construction scheme solves the problem of water flow in front of the wharf.

The Maji Mountain has excellent water depth condition for port construction. The current speed in front of the port can reach to around 200 cm/s. The influence of the Phase III project on the surrounding environment is relatively limited. Through numerical simulation and sedimentation calculation, it is clear that the siltation in the entire project area is not a big concern. However, since the wharf and the coastline formed a semi-enclosed inner bay, the weak current may cause the siltation there. So it is recommended a regular depth monitoring and dredging as well as other countermeasures.

Taking typhoon “Canhong” as an example, the model results show that the siltation rate is less than 0.025 m/d during storm in MMP waters, so there is no possibility for sudden siltation. It is also suggested that the observation on sedimentation and flow movement during storms should be further strengthened, in order to better understand the impact of storm on sediment transport.

References

Chen Changsheng, Beardsley R C, Cowles G. 2006. An unstructured grid, finite-volume coastal ocean model (FVCOM) system. Oceanography, 19(1): 78–89

Cui Zheng, Xu Xiao, She Xiaojian, et al. 2008. Analyses on flow condition along extended Majishan unloading harbor in Bao Steel. Hydro-Science and Engineering (in Chinese), (4): 32–38

Feng Haifang, Kuang Cuiping, Liu Shuguang, et al. 2008. Numerical simulation and analysis of the effect of Huanghua harbour on tidal flow. Journal of North China Institute of Water Conservancy and Hydroelectric Power (in Chinese), 29(4): 20–24

Fu Gui, Li Jiufa, Dai Zhijun, et al. 2007. Study of tidal flow numerical simulation on the reclamation project of Nanhuizui beach. Transactions of Oceanology and Limnology (in Chinese), (4): 47–54

Gao Feng, Zhang Hongyang, Liu Haicheng, et al. 2010. Numerical modeling of tidal current and sediment of reconstruction and extension projects of wharf in Beilun power plant. Journal of Waterway and Harbor (in Chinese), 31(1): 12–19

Ji Rongyao, Lu Yongjun, Zuo Liqin. 2015. The sea engineering hydrodynamic impact study of Shengsi center fishing port. In: Zuo Qihua, Dou Xiping, eds. The Seventeenth China Ocean (Shore) Engineering Symposium (in Chinese). Beijing: China Ocean Press

Liu Zhongjun, Liu Aizhen, Yu Kechen. 2012. Influence of land reclamation on hydrodynamic environment in Tianjin area. Journal of Waterway and Harbor (in Chinese), 33(4): 310–314

Liu Jiaju. 2012a. A unified computation method of siltation for dredged approach channel in different sediment beaches. The Ocean Engineering (in Chinese), 30(1): 1–7

Liu Jianqiang. 2012b. Mumerical study on the environment effects of marine engineering on the mouth of Xiaoqing River in Laizhou Bay (in Chinese) [dissertation]. Qingdao: Ocean University of China

Liu Xiao, Feng Xiuli, Liu Jie. 2016. Hydrodynamic evolution characteristics of southwest Laizhou Bay under the effect of port construction. Marine Sciences (in Chinese), 40(3): 138–145

Song Dehai, Bao Xianwen, Zhu Xueming. 2009. Three-dimensional numerical simulation of tidal current in Qinzhou Bay. Journal of Tropical Oceanography (in Chinese), 28(2): 7–14

Wang Hongli, Liu Xiaoyu, Hai Reti. 2006. Effects of ironstone harbour on environmental characteristics of sea area—a case of Majishan ironstone transfer harbour. Environmental Science & Technology (in Chinese), 29(S1): 102–104

Wang Jianfeng. 2014. Impact of diversion dike in Yangshan Western Port upon flow field and sediment transport (in Chinese) [dis-

sertation]. Nanjing: Hohai University

Wen Chunpeng, Liu Tao. 2015. Numerical study on the effect of breakwater construction on tidal flow and sediment. In: Proceedings of the 6th International Conference on Intelligent Systems Design and Engineering Applications. Guiyang, China: IEEE, 538–541

Xie Jie. 2011. Numerical simulation of tidal current and sediment in Tieshan port district. Port & Waterway Engineering (in Chinese), (3): 1–9

Zhang Shenyang, He Wenliang. 2013. Tidal current analysis of Majishan harbor. Zhejiang Hydrotechnics (in Chinese), 41(5): 23–24

Zhang Wei, Liu Ran, Qian Wei, et al. 2014. Influence of large-scale coastal engineering on hydrodynamics and sediment transport. Journal of Waterway and Harbor (in Chinese), 35(1): 1–7

Zhu Junzheng, Cao Ying. 2010. Application of FVCOM for computation of 3D tidal flow and salinity in Xiangshan Bay. Marine Environmental Science (in Chinese), 29(6): 899–903